processes

Article

Mechanism Analysis and Potential Solutions for Casing Deformation of Shale GAS Fracturing Wells in Sichuan Basin

Bihua Xu [1], Shuo Yang [1], Bin Yuan [1,*], Lu Ma [2] and Leding Wang [2]

[1] State Key Laboratory of Oil and Gas Reservoir Geology and Exploitation, Southwest Petroleum University, Chengdu 610500, China
[2] Sichuan Shale Gas Project Management Department, CNPC Bohai Drilling Engineering Company Limited, Chengdu 610057, China
* Correspondence: 202199010013@swpu.edu.cn

Abstract: Casing deformation caused by fault and fracture sliding derived from fracturing has attracted growing attention. Casing deformation frequently occurs during the hydraulic fracturing process in the Sichuan Basin. Although its mechanism has been intensively studied, this issue is becoming increasingly severe and demands immediate solutions, especially in the shale gas blocks of Changning-Weiyuan-Zhaotong. The present study summarizes and analyzes the research progress relevant to casing deformation based on the existing literature. It is shown that the casing deformation rate of the deflection point on the shale gas horizontal well is much higher than that of other places and that shear deformation is the dominant form. The main factors influencing the casing deformation of shale gas horizontal wells include weakened strength of the collapsing casing, geological factors, cement, cement quality sheath, fracturing engineering factor, etc. We propose to reduce casing deformation by optimizing well trajectory, improving casing strength and cementing quality or optimizing fracturing operation. In addition, a hierarchical relationship between the influencing factors is also provided. However, the mechanisms of some forms of casing deformation need to be further studied, and the casing deformation in shale gas exploitation must be solved urgently.

Keywords: casing deformation; hydraulic fracturing; shale gas horizontal well; Sichuan Basin; countermeasures

check for updates

Citation: Xu, B.; Yang, S.; Yuan, B.; Ma, L.; Wang, L. Mechanism Analysis and Potential Solutions for Casing Deformation of Shale GAS Fracturing Wells in Sichuan Basin. *Processes* **2022**, *10*, 1711. https://doi.org/10.3390/pr10091711

Academic Editors: Tianshou Ma, Yuqiang Xu and Albert Ratner

Received: 14 June 2022
Accepted: 20 August 2022
Published: 27 August 2022

1. Introduction

The Sichuan Basin is a typical shale gas production base in China. There are many famous shale gas blocks, such as the well-known Jiaoshiba [1–3], Changning-Weiyuan [3–5], and Fushun-Yongchuan blocks [6]. The permeability and porosity of the shale matrices are very low [7], but their natural fractures and bedding planes make them worth exploiting commercially [8,9]. However, the conventional depressurization production used in sandstone and carbonate reservoirs is no longer suitable for shale gas [8,9]. To achieve commercial exploitation, long horizontal wells combined with massive multistage hydraulic fracturing technology are employed to communicate natural fractures and bedding planes to form a fracture network [10–12].

The longer horizontal segment of a well passes through a reservoir with different mechanical properties, which results in a non-uniform stress distribution on the horizontal segment [13]. Furthermore, multistage fracturing operations cause drastic changes in the pressure and temperature of the casing [14,15]. The casing of a horizontal segment is easily deformed and damaged in a complex mechanical environment [16,17]. The casing deformation renders it difficult for bridge plugs to pass the deformation section, which significantly impacts subsequent simulation operations and production efficiency, even leading to the well's retirement before the fracture operation's completion [18–20].

Casing deformation during fracturing is a common issue in shale gas horizontal wells in the Sichuan Basin, and especially in the Changning-Weiyuan shale gas block. Although shale gas development is a mature technology in China, casing deformation causes delays in its exploration. To explain why its occurrence happens in shale reservoirs, researchers have investigated factors that may lead to casing deformation, including casing strength reduction, geological and fracturing engineering factors, etc. [14,21–25]. Hence, there is a need to research and analyze recent progress and developments in the study of casing deformation in shale reservoirs.

This paper studies the development of casing deformation concerning developments and problems arising from casing deformation in order to provide technical support for shale gas production. The first part of the research focuses on casing deformation characteristics. The third section analyzes the internal relationship between each influencing factor and casing deformation. Both historic and newer methods proposed for studying casing deformation are analyzed. In the third section, the internal relationship between each influencing factor and casing deformation is analyzed. In the fourth section, the countermeasures to casing deformation are summarized. Finally, casing deformation in Lu 203H60-3 well was analyzed, and future development will be prospected.

2. Casing Deformation Characteristics

2.1. Frequent Occurrence

Statistics show that casing deformation is a widespread and prominent problem in Sichuan Basin (Figure 1). By March 2022, 993 horizontal wells were fractured in the Changning-Weiyuan-Zhaotong shale gas block, and the casing deformation occurred in 269 Wells; the deformation rate is 26.93%. The casing deformation ratio of the Changning, Weiyuan, and Zhaotong shale gas wells reached 21.51% (77/358), 48.75% (136/279), and 24.65% (53/215), respectively. The casing deformation ratio was only 18.75% (3/16) in the Yongchuan shale gas block. Only 800 wells had casing deformation in the Fuling shale gas block [18]. These data indicate that casing deformation is more serious and frequent in the Changning and Weiyuan shale gas blocks than at Yongchuan and Fuling.

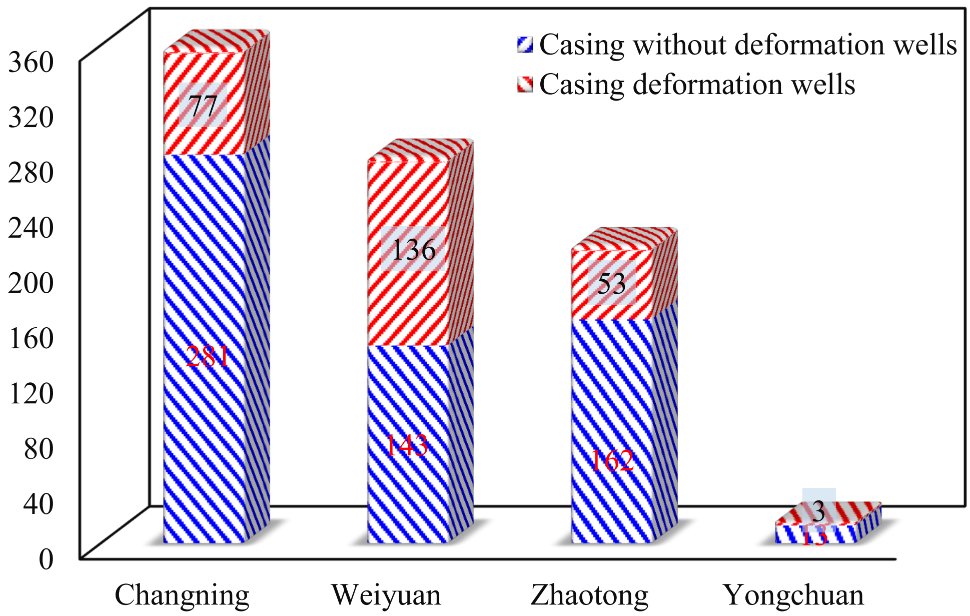

Figure 1. Statistics on casing deformation in some shale gas fields of Sichuan Basin.

2.2. Distribution Characteristics of Deformation

According to the statistics on casing deformation positions, the number occurring at target "A" is higher than 47.0% in the Changning-Weiyuan [18,19] and 43.8% in the Weiyuan-Rongxian shale gas areas (Figure 2). In Changning-Weiyuan, 65.0% of deformation points were located near the heel and 29.0% between the heel and toe. Figure 2 shows that others occurred at the toe [20]. The following aspects summarize the distribution characteristics of casing deformation:

(1) The deformation points increased from the toe to the heel of a horizontal well.
(2) The number of casing deformation points within 200 m of the target "A" was much higher than others.
(3) Most of the casing deformations occurred after the operation of several fractured segments or during the drilling of the bridge plug.
(4) The damage extent of deformation points increased with the fracturing operation time.
(5) The number of deformation points near natural fractures and faults was much higher than others.

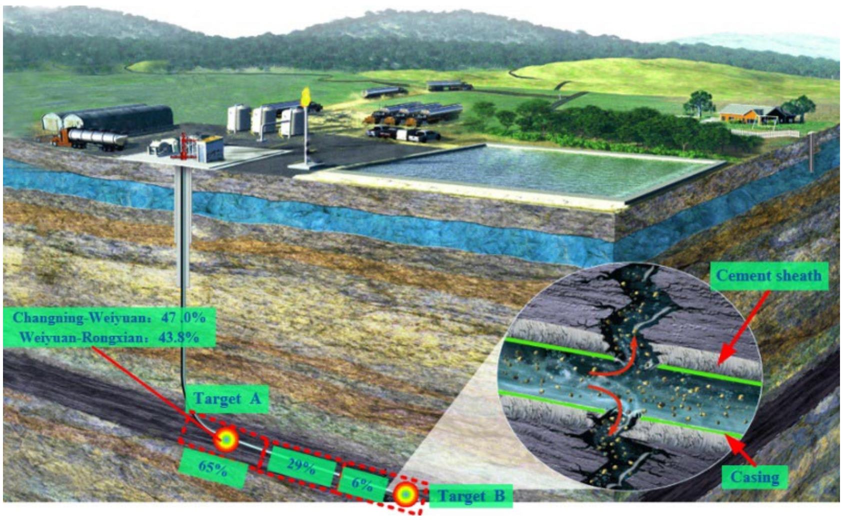

Figure 2. Distribution of casing deformation points of shale gas horizontal well in Sichuan Basin.

2.3. Deformation Morphology

The statistical results show that shear deformation and collapsing deformation are the primary forms of casing deformation [26–28]. Three-dimensional logging imaging of casing in the Changning-Weiyuan area shows that most casing deformations are shear deformations [16,21]. Shear deformation was induced by fracture/fault slip and nonuniform loads on casing during hydraulic fracturing [22,23]. However, a stereotypical test of shale gas wells in the Fuling area indicated that the casing deformation was dominated by collapsing deformation [18]. This may be due to the fact that the geological structure of the Fuling area is more stable, and there is no fracturing-induced fracture/fault slip. In addition to shear and collapsing deformation, there was also a small amount of bending deformation and axial "S"-shaped deformation owing to casing "hanging" during fracturing in Sichuan Basin. These two deformations are mainly due to the well trajectory and casing strength.

3. Casing Deformation Influence Factors

3.1. Casing Collapsing Strength Reduction

The burial depth of shale reservoirs in the Sichuan Basin ranges from 2000 m to 6000 m [6], and the reservoir temperatures range from 50 °C to 130 °C [24]. Furthermore, the casing collapsing strength is reduced by worn, bending, temperature, and perforation. [25]. The casing collapsing strength is reduced by wearing, bending, temperature, and perforation.

3.1.1. Bending Reducing Casing Collapse Strength

The trajectory of a horizontal well cannot remain horizontal in a horizontal segment, and there are many curved sections. Furthermore, the casing in the building angle section is also bending. A dogleg angle will increase the casing bending stress and weaken the casing collapsing strength. It was found in experiments when the dogleg angle was 7°/30 m. The casing collapsing strength decreased from 73.8 MPa to 61.2 MPa for a TP110-grade casing [26]. The curvature also increased the wear of the casing and the eccentricity, which are additional factors that affect the casing deformation. The bending of the casing explains the reason for the high deformation rate of the casing near the "A" target point.

3.1.2. Temperature Reducing Casing Collapse Strength

High temperature or dramatic temperature fluctuations will reduce the casing collapsing strength [20,27]. The casing collapse strength decreases at high temperatures; the reduction law can be described by Equation (1) [28]. When the casing is in a 100 °C environment, its strength decreases by 4.32%. Due to the effect of thermal expansion and cold contraction, a rapid temperature decrease causes axial stress in the casing, thus reducing its collapsing strength [24,29]. For the type-TP110 casing, the casing strength decreases by 14% when the temperature is lowered by 70 °C. For TP140, the strength is reduced by 10% [29]. Sudden reductions in temperature also lead to annulus fluid shrinkage, increasing the casing stress [14]. Therefore, Kaldal, Jonsson [27] think that the influence of temperature on the casing collapsing strength was considered one of the main factors. However, this view has not been proven.

$$\sigma_{Temp} = [1 - 0.00054(T - 20)]\sigma_{20}. \tag{1}$$

where σ_{Temp} is the casing collapsing strength at high temperature, MPa; T is the temperature, °C; σ_{20} is the casing collapsing strength at 20 °C.

3.1.3. Wore Reducing Casing Collapse Strength

During drilling and hydraulic fracturing operations, the drilling strings, coiled tubing, and other tools easily rub against the casing in curved sections, resulting in wearing on the casing [25]. According to field caliper logging data, the casing wear rate is as high as 12.0%. Stress concentration occurs after casing wear, and the wear depth increases with the dogleg [22]. A worn casing is more susceptible to deformation under the coupling of temperature and nonuniform stress [30], especially at target "A" [19]. The bending of the wellbore trajectory causes casing wear, so casing bending and casing wear will coincide. Therefore, the combined effect of bending and wear is an essential factor that induces the deformation of the casing.

3.1.4. Perforation Reducing Casing Collapse Strength

A perforation will destroy the integrity of the casing structure and cause stress concentrations at the perforation holes. At the same time, perforations will cause the casing to crack. A casing with multicluster perforation was placed in complicated stress conditions during fracturing operations [31]. However, Zhao [32] and Xi, Li [19] found that casing deformation did not occur at the perforation position even though casing deformation is the most serious at Changning-Weiyuan.

3.2. Geological Factors

3.2.1. In-Situ Stress

The in-situ stresses in three directions are rarely equal, so the casing is always under nonuniform stress. When the horizontal segment of a shale gas well is under nonuniform in-situ stress, the casing is subjected to shear stress from the in-situ stress [33]. Furthermore, multistage hydraulic fracturing changes the in-situ stress, increasing the heterogeneity of the in-situ stress and thus making it easier for the casing to collapse [31]. Stress shadows will form during multistage hydraulic fracturing as the in-situ stress gradually increases from toe to heel. Therefore, casing collapse failure often occurs quickly under high in-situ stress, especially at target "A" [34]. Table 1 lists the in-situ stresses of typical blocks in the Sichuan Basin. Changning—Weiyuan is an anticlinal—synclinal slope zone and extrusion structure, and the difference in horizontal crustal stress is significant, while Fuling Jiaoshiba is a tension-extrusion anticline structure, and the contrast of horizontal crustal stress is slight. This is one of the reasons why the casing deformation rate of the Changning-Weiyuan block is much higher than that of the Fuling block.

Table 1. Comparison of in-situ stress in typical blocks of Sichuan Basin.

Well No.	Maximum Horizontal Principal Stress (MPa)	Minimum Horizontal Principal Stress (MPa)	Horizontal Stress Difference (MPa)	Coefficient of Horizontal Stress Difference
Wei 202	70.0	54.0	16.0	0.296
Wei 204	88.3	69.6	18.7	0.269
Ning 201	57.0	44.6	12.4	0.278
Jiao 1	54.0	49.0	5.0	0.102

3.2.2. Fracture/Fault Slip and Lithological Interface

Many faults, natural fractures, lithologic interfaces, and beddings in shale reservoirs are basic conditions for commercial exploitation [17]. However, during multistage hydraulic fracturing, the in-situ stress balance near the wellbore is destroyed owing to a large amount of injected fracturing fluid. Then, the faults, natural fractures, lithologic interfaces, and beddings are prone to slipping. This can cause casing shear deformation [20,23]. The non-uniform distribution of natural fractures in space and the heterogeneity of in-situ stress are other factors that lead to slippage [35]. A statistical analysis of the geological conditions of deformation points using seismic and logging data showed that about 61.7% of the total casing deformation points were related to fractures/faults and lithologic interfaces/bedding [18,21]. In a numerical simulation, Guo [36] found that casing deformation dramatically increases with the fracture/fault slip distance. About 52.38% of the casing deformation points were located in the lithologic interface area, according to statistics by Chen, Shi [21] and Xi, Li [18]. The casing deformation locations in different blocks are shown in Figure 3. Statistics show that 80% of casing deformation risks in Luzhou block are located at the natural fractures and bedding interface, and nearly 50% of casing deformation sections in Weiyuan block fractures developed. Therefore, fracture/fault slip and lithological interfaces are significant causes of casing deformation in Changning-Weiyuan-Rongxian-Luzhou shale blocks [19,37].

3.2.3. Microseism

Multistage hydraulic fracturing can induce microseisms [38]. For example, hydraulic fracturing triggered earthquakes in western Canada, and the most significant moment of magnitude was 3.9 [39]. Changning-Weiyuan-Rongxian-Luzhou is located in a geologically active area. However, the geological structures of Fuling and Yongchuan are relatively stable. During massive multistage hydraulic fracturing, microseism is easily triggered, thus increasing the slip distance of fractures/faults. Figure 4 shows the microseism and impacts before and after fracturing in different blocks. Microseism is the inducing factor of fracture/fault slip, and the real cause of casing deformation is still fracture/fault slip. Therefore, deformation in Changning-Weiyuan-Rongxian-Luzhou is more serious than in Fuling and Yongchuan.

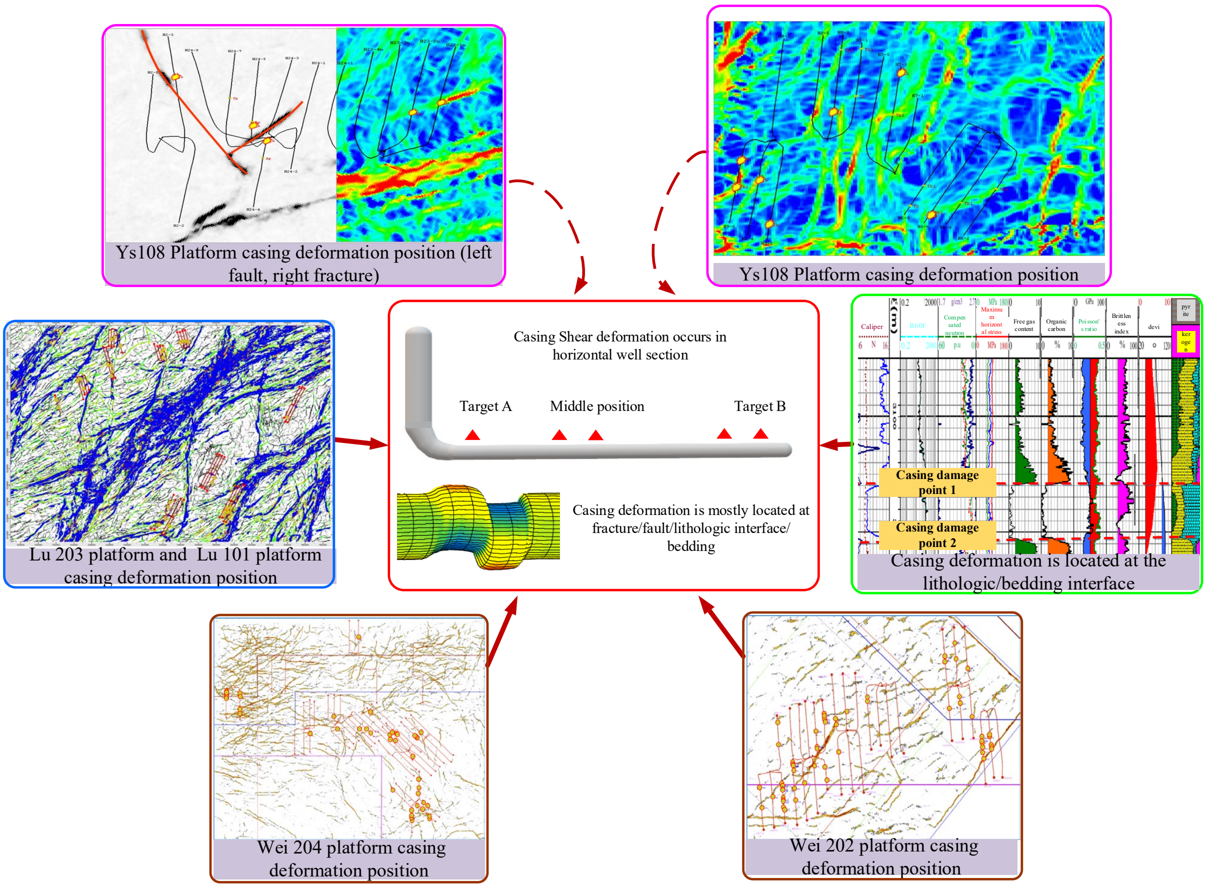

Figure 3. Location of casing deformation in different blocks.

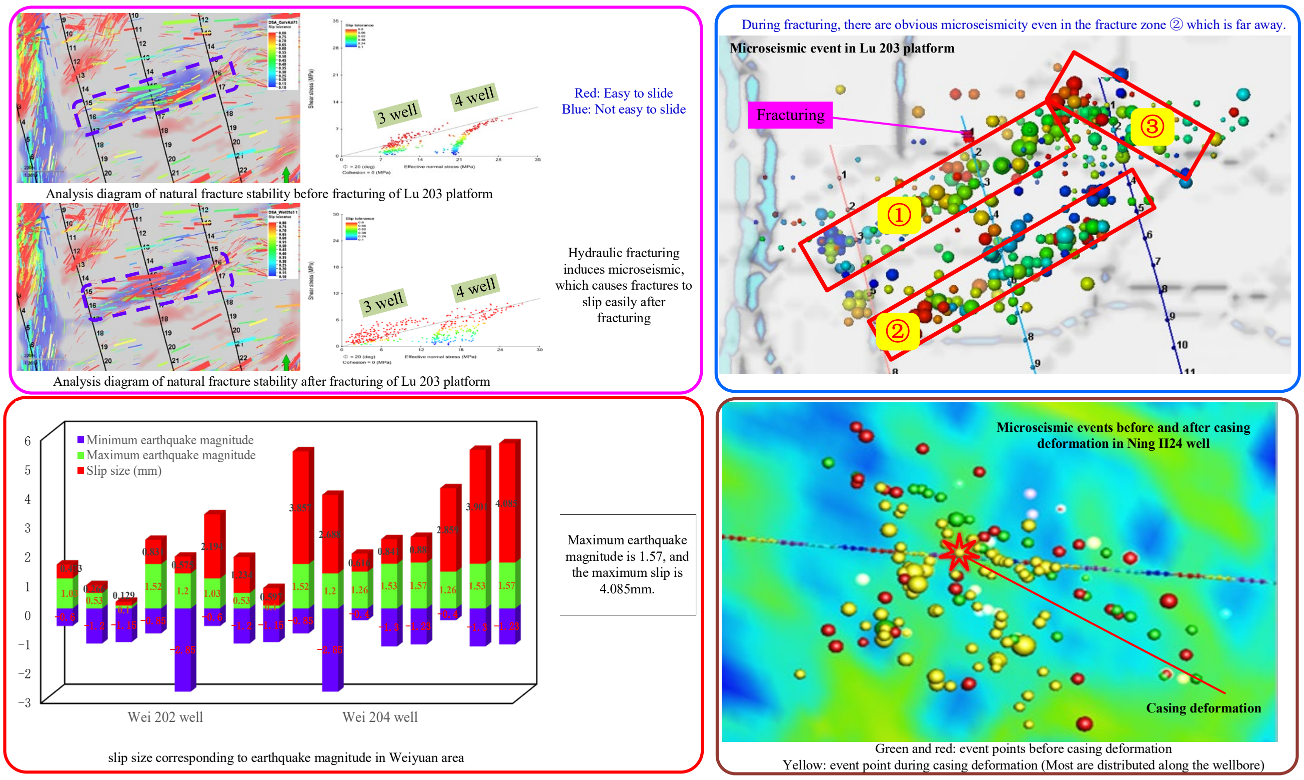

Figure 4. Microseismic events and their effects before and after fracturing in different blocks.

3.2.4. Shale Swelling

In the process of producing shale gas by fracturing, the water and ions from fracturing fluid enter the shale, causing the shale to absorb water and expand and changing the stress distribution of the casing [37]. Some studies have shown that the casing stress is 500 MPa when there is no shale expansion, while it increases to 1100 MPa when the shale expansion rate is 0.4% [40]. Figure 5 shows the impact of shale swelling on fractures and casing. Due to hydraulic fracturing, many artificial fractures are formed, and some natural fractures are connected, resulting in a significant increase in the contact area between fracturing fluid and shale. This may be one of the reasons why the number of casing deformations near the natural fracture is much more than in other locations.

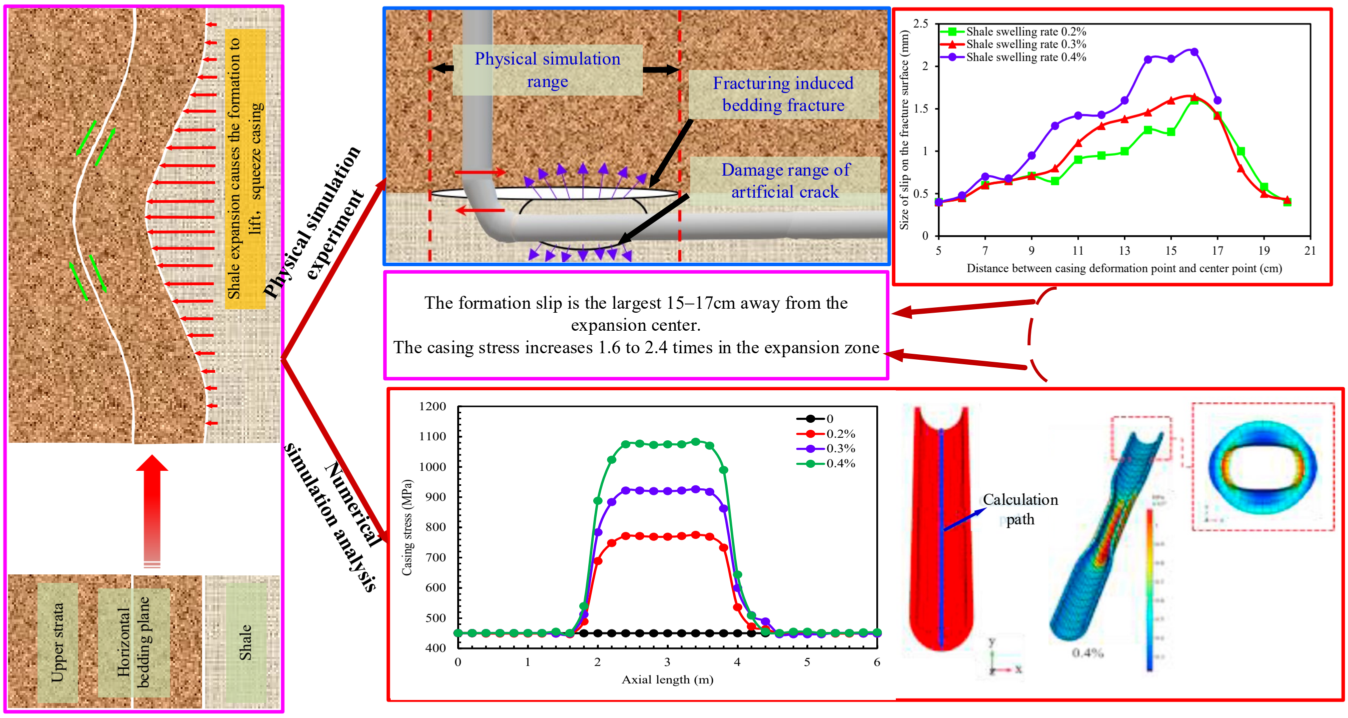

Figure 5. Effects of shale swelling on fractures and casing (numerical simulation from Li [41]).

3.3. Casing Eccentricity

Casing weight, the collapse of the well wall, and improper positioning of the centralizer resulting in casing eccentricity easily occur in the buildup and horizontal segments in cementing horizontal shale gas wells [42]. Casing eccentricity leads to a heterogeneous distribution of the annulus velocity of the cement slurry during cementing, resulting in rate efficiency at narrow gaps. This easily leads to cement sheath voids and channeling [43]. Figure 6 shows that when the centering degree of the casing is 67%, the outer extrusion stress of the casing is more significant, and the cement sheath is damaged at the thinnest part. An eccentric casing is easily deformed owing to the mechanical-thermal coupling effect [40].

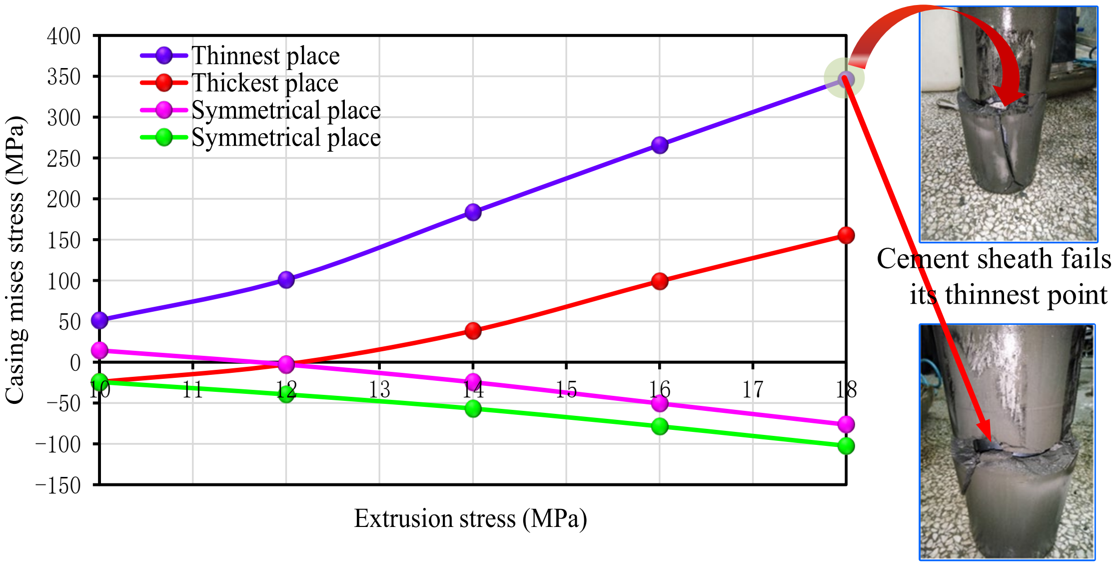

Figure 6. Casing mises stress distribution when 67% casing is centered.

3.4. Cement Quality and Cement Sheath Properties

A horizontal segment is long, and it is not difficult to achieve good cement quality. Poor cement quality is one factor that causes casing deformation in shale gas horizontal wells [44]. Poor cement quality is characterized by the poor quality of cementation, cement sheath voids, and channeling in the annulus [19,33]. Poor cement quality combined with the asymmetry of the fracturing area results in more serious casing deformation. Furthermore, the mechanical properties and thickness of the cement sheath also affect the casing deformation [19,45]. Figure 7, an experiment conducted in our laboratory, shows the effects of casing center degree, cement elastic modulus, cement gas penetration length, and missing cement thickness on casing circumferential stress.

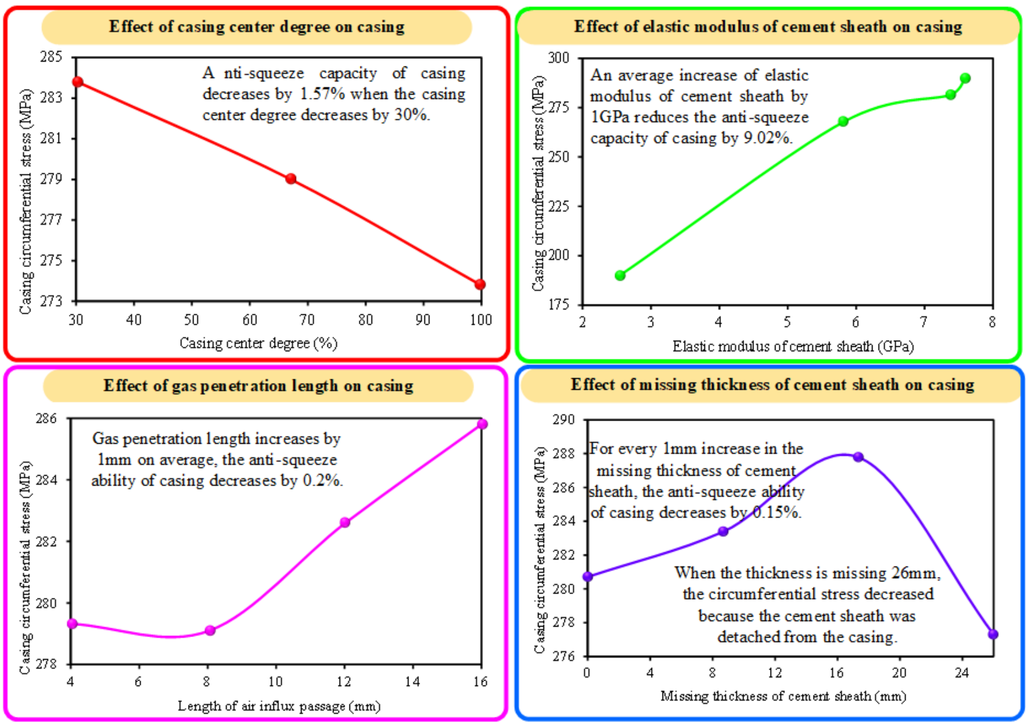

Figure 7. Relationship between casing circumferential stress and quality, performance of cement sheath.

3.4.1. Cement Sheath Voids and Channeling

Channeling and voids frequently occur in shale gas horizontal wells owing to eccentricity and low rate efficiency. The casing is under nonuniform stress, and when the cement sheath contains voids, a phenomenon similar to "annular pressure buildup" appears [14,33]. A cement void amplifies the nonuniform stress on the casing, thus increasing the casing shear stress, which causes casing shear deformation.

The geometry of cement sheath voids also affects the casing stress since it affects the stress distribution on the casing [14,44]. Research results showed that the casing stress increases and decreases with the void angle, reaching its maximum value when the void angle is 45° [40]. The injection of a large amount of cooling fracturing fluid into the casing resulted in a significant reduction in the internal pressure of the cement sheath voids. The loss in pressure can be expressed as follows [14]:

$$p_{loss} = \left(\frac{\Delta T \alpha}{B_N} \right) \tag{2}$$

where B_N is the fluid compressibility, m^2/N; α is the fluid thermal expansion coefficient, $1/°C$; and ΔT is the reduction in temperature, °C.

The casing partly lacks external support when the fluid pressure is deficient in the voids. Under the combined effect of high internal pressure and asymmetrical external supporting force, plastic deformation will occur on a casing as the stress concentration increases. Near the target "A", cement sheath voids occur easily owing to the curved wellbore trajectory and sudden temperature changes. Therefore, filling the annulus with a cement slurry to ensure cementing quality is one of the necessary conditions for reducing casing deformation.

3.4.2. Properties of Cement Sheath

The mechanical properties of a cement sheath (compressive strength, bonding strength, Young's modulus, Poisson's ratio, etc.) affect the stress on the casing. With a decrease in Young's modulus of a cement sheath, the maximum casing stress decreases sharply [45,46]. For a TP140-grade casing, its safety coefficient improved from 0.98 to 1.2 when Young's modulus of the cement sheath was reduced from 10 GPa to 5 GPa [20]. Shale is generally hard and brittle and has a high Young's modulus [47]. Suppose Young's modulus of a cement sheath is close to that of formation (high Young's modulus). In that case, the in-situ stress is more easily and efficiently transmitted to the casing, resulting in deformation.

A cement sheath with a low Young's modulus and high Poisson's ratio can significantly reduce the radial and tangential stresses of the cement sheath, thereby promoting integrity in the cement sheath [46]. Improving the integrity of a cement sheath can reduce local stress on the casing and fluid channeling in the annulus, thus reducing the volume of bound fluid in the annulus [14]. Moreover, an integrated cement sheath can reduce the casing deformation lowering the temperature and pressure changes of the bound fluid in the annulus.

3.4.3. Cement Sheath Thickness

Increasing the thickness of the cement sheath involves adding more stress-absorbing materials between the formation and casing, thereby reducing the effect of in-situ stress on the casing. The casing stress decreased slightly with an increase in the cement sheath thickness during faults/natural fracture slippage [20]. Increasing the thickness of the cement sheath involves adding more stress-absorbing materials between the formation and casing, thereby reducing the effect of in-situ stress on the casing. However, the thickness of the cement ring has a limited effect on casing deformation compared to other influencing factors [48]. Only considering increasing the thickness of the cement sheath cannot solve the problem of casing deformation.

3.5. Alternating Temperature and Pressure

There are alternating internal pressure and temperature during the multistage fracturing, which affects the casing deformation in two ways. On the one hand, the coupling of alternating temperature and pressure imposes alternating stress on the casing [30]. Under the alternating stress, the cement sheath is easily peeled from the casing to form a micro gap [14]. On the other hand, they will break down the integrity of the cement sheath sealing, thus forming a micro-annulus in the casing-cement formation [49], increasing the amount of annular fluid. If the alternate stress exceeds the yield strength of the casing, the yield strength of the casing decreases with the increase in the number of alternations [18]. The relationship between temperature and safety factor of casing triaxial in the Changning-Weiyuan area is analyzed, and Wei202 well is taken as an example. Under a small temperature range, the casing compressive strength is affected to a certain extent (Figure 8). The effect of the cement-sheath-sealing integrity on the casing deformation is similar to that of a cement sheath void on a local load. The casing at target "A", with the lowest collapsing strength under the most significant number of cyclic loads, was more prone to deformation. Therefore, the abrupt temperature change during fracturing was considered one of the main factors resulting in casing deformation [50].

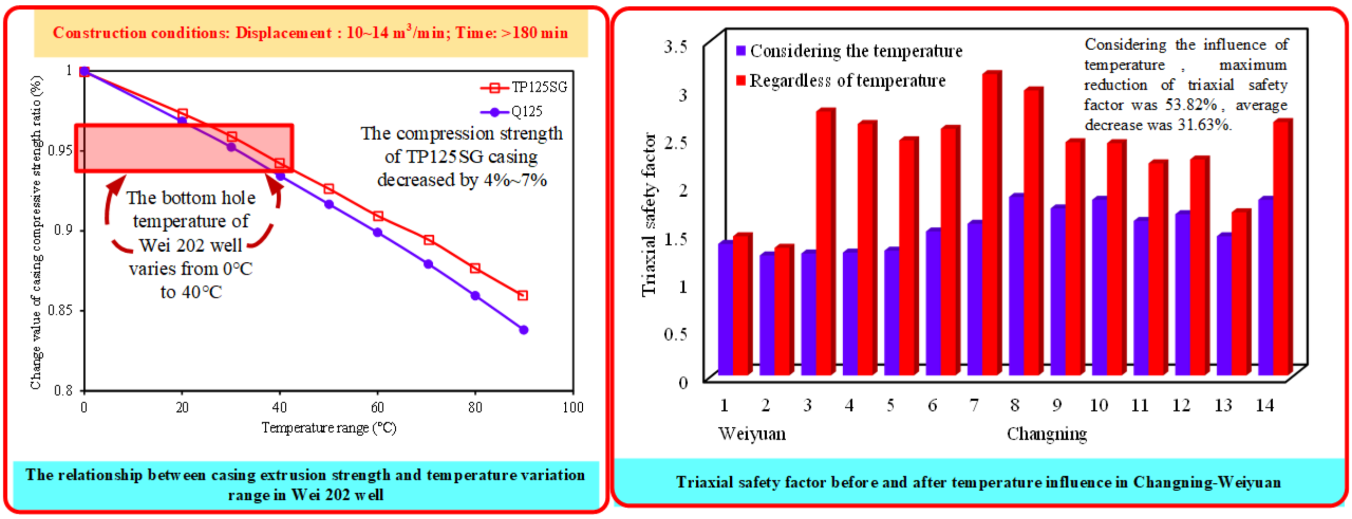

Figure 8. Relationship between temperature and casing strength.

3.6. Hydraulic Fracturing Parameters

3.6.1. Injection Rate

One of the characteristics of multistage hydraulic fracturing is that each stage injects thousands of cubic meters of liquid at a pump rate of over 10 m^3/min at a high pump pressure [51]. Figure 9 shows the fracturing injection rate of nine deformed casing Wells in Weiyuan, with an average maximum injection rate of 14 m^3/min. When there is bound fluid in the annulus, the temperature of the bound fluid within the cement sheath void will continue to decrease as the fracturing fluid is continuously injected. Then, the pressure of the cement-sheath void segments drops sharply [24]. With an increase in the rate, the maximum temperature difference increases continuously from heel to toe [24,29]. The casing stress increases with the injection rate. In addition, a higher injection rate can increase the influence of stress accumulation [37]. Therefore, the deformation risk of the casing increases with the injection rate [31].

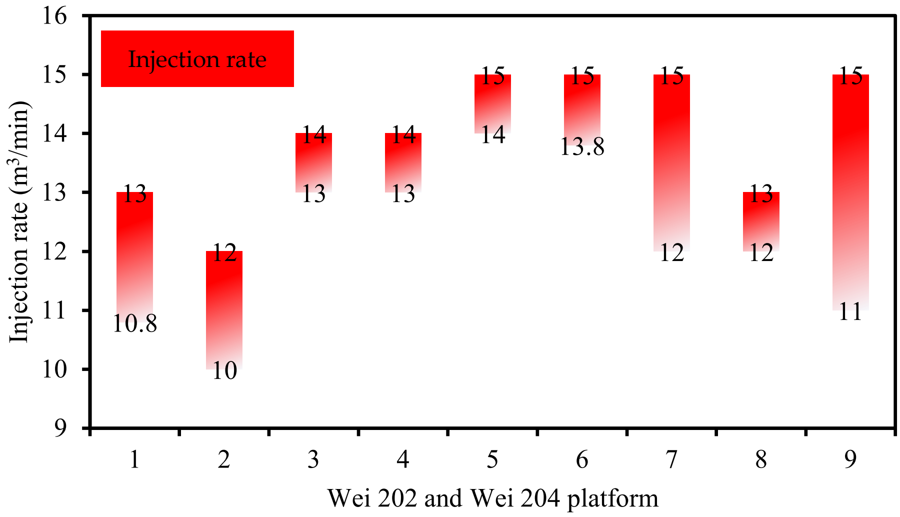

Figure 9. Fracturing injection rates of nine casing deformation wells in the Weiyuan area.

3.6.2. Injection Pressure

High injection pressure is needed during multistage hydraulic fracturing to break up shale reservoirs to form fracture networks. Figures 10 and 11 show the fracturing injection pressure of some casing deformation Wells in the Changning-Weiyuan area. The average injection pressure was 76.2 MPa on Chang 201 platform and 81.7 MPa on Wei 204. When the casing is under nonuniform loading, it is challenging to avoid casing deformation when improving its grade. As a cement sheath is integrated, the casing's internal pressure has a negligible effect on the casing stress. For example, even if the casing internal pressure reaches 110 MPa, the maximum casing stress is only 291.2 MPa [19,31]. However, once the cement sheath void is broken or the casing is under nonuniform loading, the casing stress will rapidly increase with the casing's internal pressure [19,20]. Calculations showed that when the internal pressure is 95 MPa, the casing stress could reach 1000 MPa (the yield strength of TP140 is 965 MPa) [20].

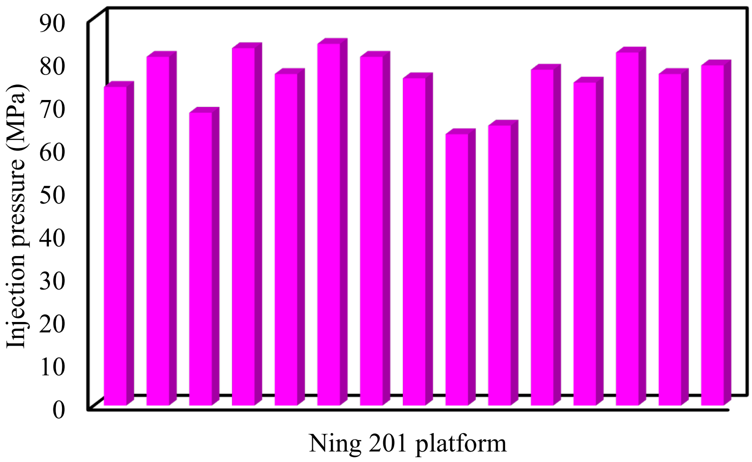

Figure 10. Fracturing injection pressure of 15 deformed casing wells in the Changning 201 platform.

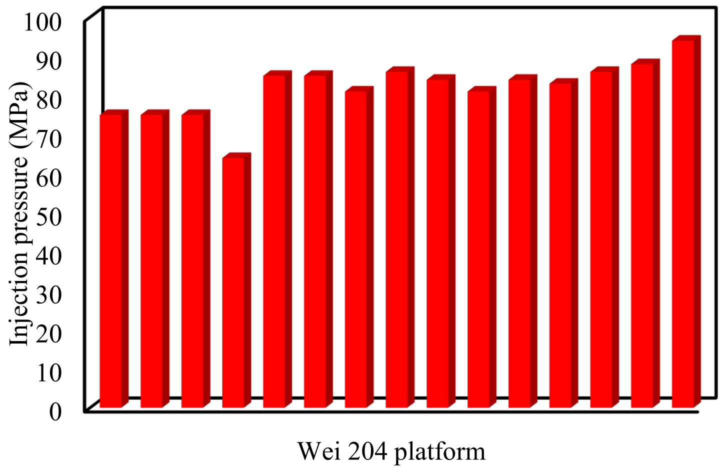

Figure 11. Fracturing injection pressure of 15 deformed casing wells in the Weiyuan 204 platform.

4. Analysis of Relationship between Influence Factors

Two or more influencing factors are required to deform the casing. Based on the frequency of casing deformation caused by these influencing factors, we have summarized the effect degree of these influencing factors, as shown in Table 2. The fracture/fault slip and microseisms are the strong influence factors and the leading cause of casing deformation. They can cause casing deformation. Casing wear, temperature, non-uniform in-situ stress, cement sheath voids and channeling, alternating temperature and pressure, injection rate, and injection pressure are medium influence factors. Only weaker influence factors cannot make casing deformation. However, if the casing has been affected by other strong or medium influence factors, weaker factors will make the casing deformation more serious.

Table 2. Effect degree of influence factors.

Influence Factors		Effect Degree of Influence Factors		
		Strong	**Medium**	**Weaker**
Casing collapsing strength reduction	Casing bending		√	
	Temperature		√	
	Casing wear		√	
	Perforation			√
Geological factors	Non-uniform in-situ stress		√	
	Fracture/fault slip and lithological interface	√		
	Microseism	√		
	Shale swelling	√		
Cement quality and cement sheath properties	Casing eccentricity		√	
	Cement sheath voids and channeling		√	
	Properties of cement sheath			√
	Cement sheath thickness			√
Fracturing engineering factors	Alternating temperature and pressure		√	
	Injection rate		√	
	Injection pressure		√	

However, the influence factors of casing deformation are not independent. The relationship between various influence factors is shown in Figures 12 and 13. The wellbore trajectory and gravity cause bending in the casing, leading to casing wear and forming a narrow eccentric annulus. Bending and casing wear lead to the collapsing strength of the casing reduces. Then, poor cement quality is inevitable due to narrow eccentric annulus, resulting in a cement sheath with voids and channels. When the cement sheath has voids and channeling, there is bound fluid in the annulus. A large amount of cool fracturing fluid injected through the casing leads to fluid pressure in the bound fluid, reducing due abrupt reduction in temperature. Therefore, there will be a significant differential pressure between the inside and outside of the casing and local loading; deformation easily happens to the casing. If the casing collapsing strength has been reduced by perforations and high temperature, deformation will likely occur under the above-complicated conditions. Furthermore, a large amount of fracturing fluid entering the formation will unbalance the in-situ stress and increase its heterogeneity. In addition, multistage fracturing induces slips in the faults and natural fractures. It also causes microseisms, which increases the slip distance in unstable formations.

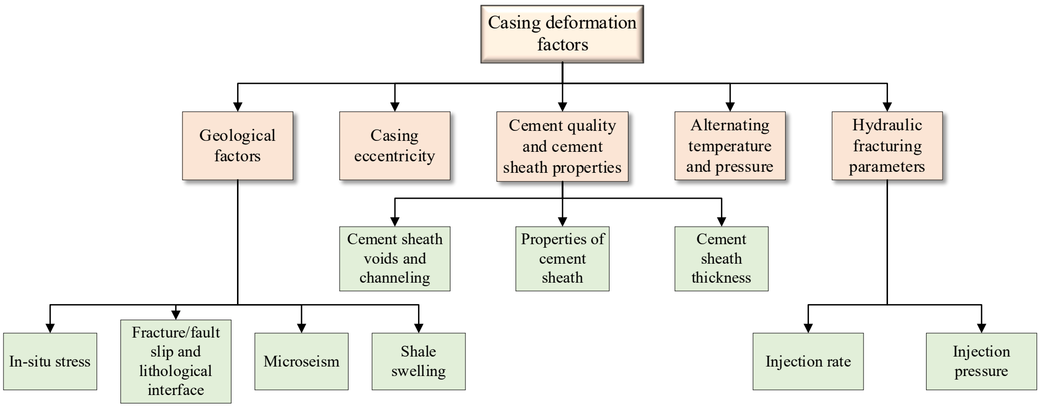

Figure 12. The relationship between the influencing factors.

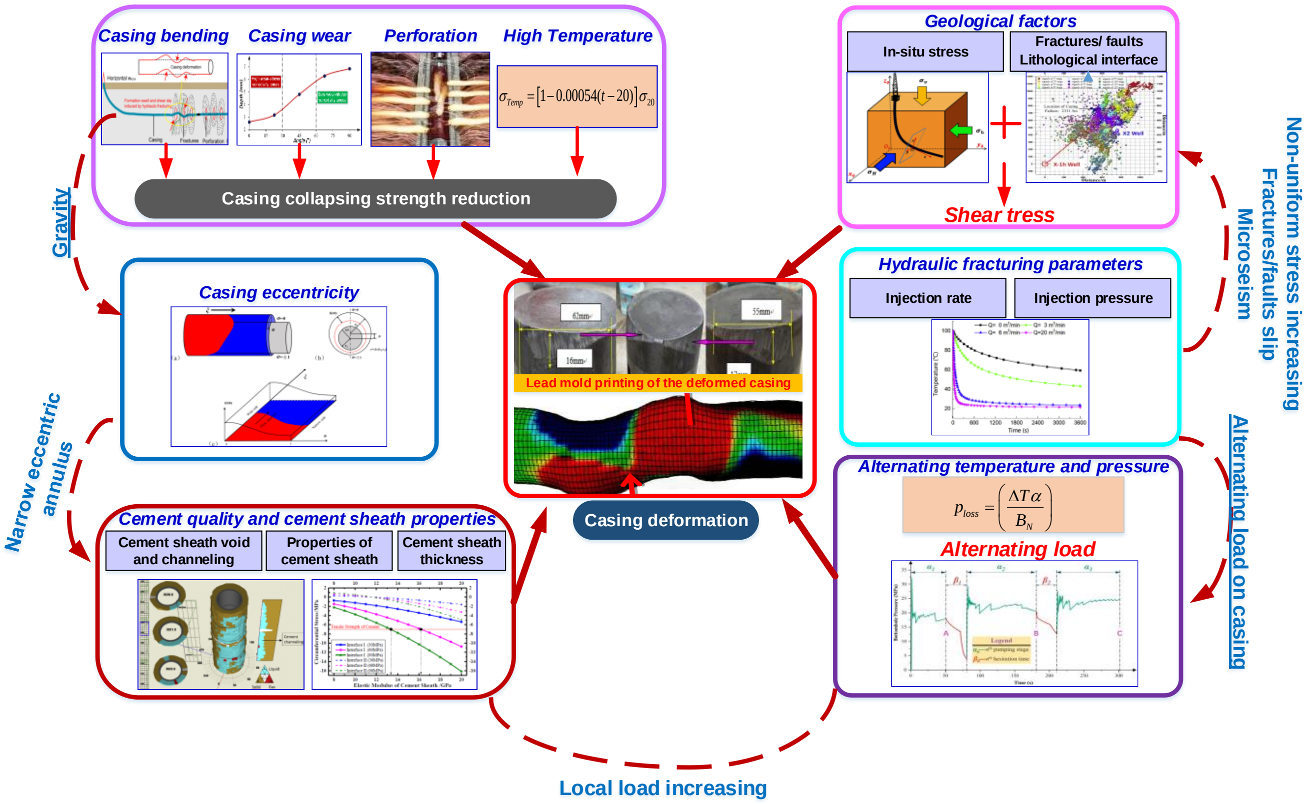

Figure 13. Schematic diagram of the relationship between various influencing factors. Some pictures in this figure from Yu [52], Xi, Li [19], Lian, Yu [31], and Liu, Gao [48].

5. Countermeasures

In studying casing deformation mechanisms and countermeasures, the researchers proposed a series of methods to prevent casing deformation, including well trajectory optimization, improving the cement quality, fracturing construction parameters optimization, casing material selection, preventing shale expansion, etc.

5.1. Optimization of Well Trajectory

Although about 61.7% of the total casing deformation points were related to fractures/faults and lithologic interfaces/bedding [18,21], these can be avoided by optimizing the wellbore trajectory design. Before optimization of the wellbore trajectory, the seismic data should be strengthened to determine the location and size of the fault to avoid shear deformation owing to the fault slip [53]. During well location selection and well trajectory design, the trajectory of the horizontal segment should avoid lithological interfaces, natural fractures, and fault development areas such as "ridges" or "valley bottoms" with severe geological structures or drill along the fracture belt [19,20]. In this way, the risk of right-angle shear casings caused by faults can be avoided, reducing casing deformation. Optimizing the wellbore trajectory can also reduce the narrow gap and casing wear caused by bending. Then, the cement quality can be improved to reduce the channeling and cement voids. In addition, the stress concentration of the casing caused by the bending stress can be reduced [45].

5.2. Optimization of Cement Sheath Properties and Cementing Parameters

In high-in-situ stress shale reservoirs, cement properties cause casing deformation [14]. Xi, Li [19] and [45] suggested that a high strength and low Young's modulus can be adopted for shale gas well cementing. Young's modulus of the cement sheath can be decreased to the maximum extent while keeping the strength is not or slightly reduced. Thus, the ability of the cement to maintain its sealing integrity can be promoted. The injection of high-viscosity fluid instead of cement was recommended since this provide space for slippage and can change the nonuniform load on the casing into a uniform load [45]. However, this method is difficult to construct, and it is difficult to find this material. The research shows that the young's modulus of foamed cement can be reduced to less than 2000 MPa [54], so foamed cement can effectively restrain casing deformation [41]. Reasonable placement of centralizers and floating casing cementing technology were adopted to improve the eccentricity of the casing to reduce channeling and voids [44]. Then, the effect of the sealed fluid pressure drop owing to the temperature drop was weakened. Yan, Zou [14] suggested that rotating the casing string during cementing can improve the cement quality and prevent cement voids' formation. In a word, shale gas horizontal wells require a high-strength and low-modulus cement slurry, and the displacement efficiency must be ensured during cementing to sure cement slurry fill the entire annulus.

5.3. Improvement Casing Strength

Maintaining the steel grade of the casing and improving its thickness, or maintaining the wall thickness of the casing and improving its steel grade, can improve the casing's collapsing resistance to reduce casing deformation [33]. In addition, it is recommended that the casing be externally thickened while maintaining the same size to reduce the impact of fracturing tools [20]. If there is a stress concentration or fracture/fault slip, reducing the casing deformation can be achieved by increasing the casing grade or wall thickness [20]. However, increasing the flexural strength by simply increasing steel grade and wall thickness cannot radically solve the failure of axial S-shaped casing deformation [31]. Moreover, increasing the casing grade or wall thickness makes it challenging to run casing. Therefore, reducing the deformation during fracturing by optimizing the casing should consider the difficulty, and other preventive measures should be considered.

5.4. Optimization of Hydraulic Fracturing Parameters

Hydraulic fracturing parameters contribute to casing deformation; thus, these parameters must be optimized. Fluid pressure in fault fractures should be controlled and reduced to reduce fault fracture activity [55], avoiding casing shear deformation. A technical scheme using a large-diameter bridge plug without drilling or a full-diameter and infinite-stage solubility ball seat seal can reduce the number of operations, reducing the casing deformation [56]. In sections with poor cement quality, the fracturing pressure should be controlled to avoid the formation of axial fractures of the cement sheath [53]. Dual or multicard packers and long-rubber-barrel packers can be installed to separate fracture zones in wells where natural fractures and beddings develop [21]. Xi, Li [19] proposed warm fracturing fluids to minimize pressure drops inside voids as an innovative strategy. However, this is difficult to achieve.

5.5. Optimization of Shale Inhibitor

Shale expansion affects casing deformation [41] significantly, and shale expansion occurs in every area in contact with fracturing fluid. Therefore, it is necessary to provide a reasonable plan to restrain shale expansion from avoiding casing deformation. High salt content is used to solve the problem of shale swelling, but it can affect the environment and fracturing fluid rheological characteristics [57]. Wang [58] proposed guar gum fracturing fluid to enhance pore connectivity, inhibit shale expansion, and improve flowback efficiency. This method can reduce the risk of casing deformation and improve the efficiency of the fracturing operation. We summarize the corresponding countermeasures for each influencing factor, as shown in Table 3. Figure 14 shows a flowchart of casing deformation countermeasures.

Table 3. The countermeasures for influence factors.

Influence Factors		**Countermeasures**
Casing collapsing strength reduction	Casing bending Temperature Casing wear Perforation	Well trajectory optimization Optimization casing strength Casing strength and well trajectory optimization Perforation parameters optimization
Geological factors	Non-uniform in-situ stress Fracture/fault slip and lithological interface Microseism Shale swelling	Casing strength optimization Well trajectory optimization Hydraulic fracturing parameters and well trajectory optimization Shale inhibitor optimization
Cement quality and cement sheath properties	Casing eccentricity Cement sheath voids and channeling Properties of cement sheath Cement sheath thickness	Well trajectory optimization Cementing parameters optimization Cement sheath properties optimization
Fracturing engineering factors	Alternating temperature and pressure Injection rate Injection pressure	Hydraulic fracturing parameters optimization

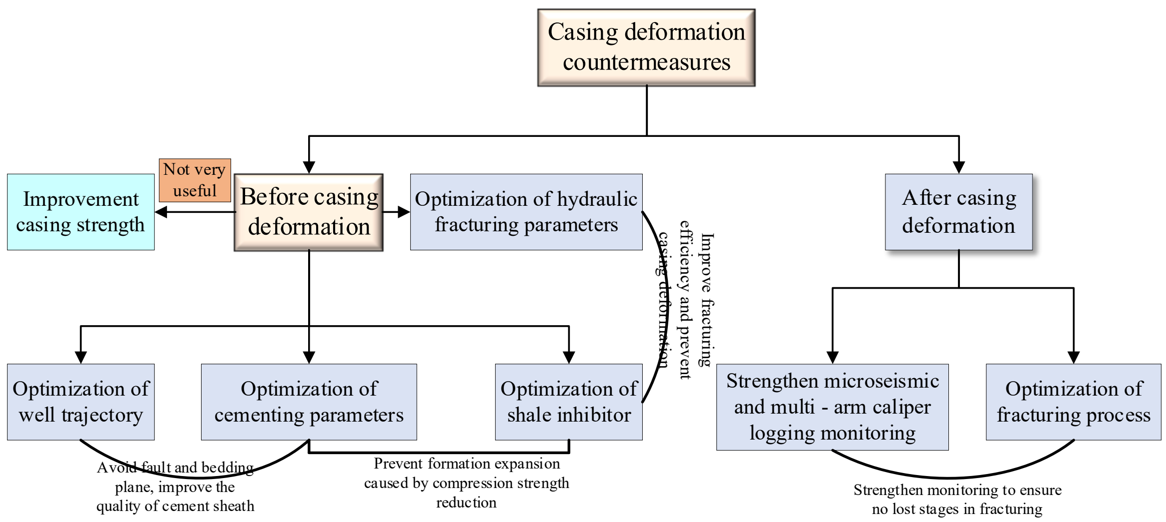

Figure 14. Countermeasures before and after casing deformation.

6. Analyze the Cause of Casing Deformation in Lu 203H60-3 Well

By February 2022, casing deformation in Luzhou 203 platform reached 48.1%. The casing deformation depth of well Lu 203H60-3 was determined through multi-arm well diameter and pumping resistance depth, and formation lithology data and construction parameters determined the cause of deformation. The multi-arm well diameter showed casing deformation at 3938.12 m, 3944.99 m, and 4012.77 m, with a maximum of 39.97 mm. While pumping 90 mm plugs to 3939.65 m and 3941.32 m in stage 22, encountered resistance. They were pumping 98 mm plug-in stage 8 encountered resistance at 4746.72 m. Figure 15 shows the well trajectory and casing deformation distribution. The five casing deformation positions measured by pumping resistance and multi-arm well diameter were identified as the same casing deformation point since 4000 m was located at the interface of the two zones, and the dogleg degree reached this point at 8.9°/30 m. A large dogleg degree specifically influences the anti-squeeze strength of the casing. In the process of multistage hydraulic fracturing, the sliding of the bedding interface and the constant change of temperature and pressure will significantly reduce the anti-squeeze strength of the casing, resulting in casing deformation. The second casing deformation location was identified at 4746.72 m. It was located near the interface between the first and second zones, and fractures developed. Acoustic cementing showed good cementing quality, but the casing deformation still occurred since the bedding and fractures during hydraulic fracturing were sliding to damage the cement sheath. The pressure difference between the casing and the casing is 80~90 MPa.

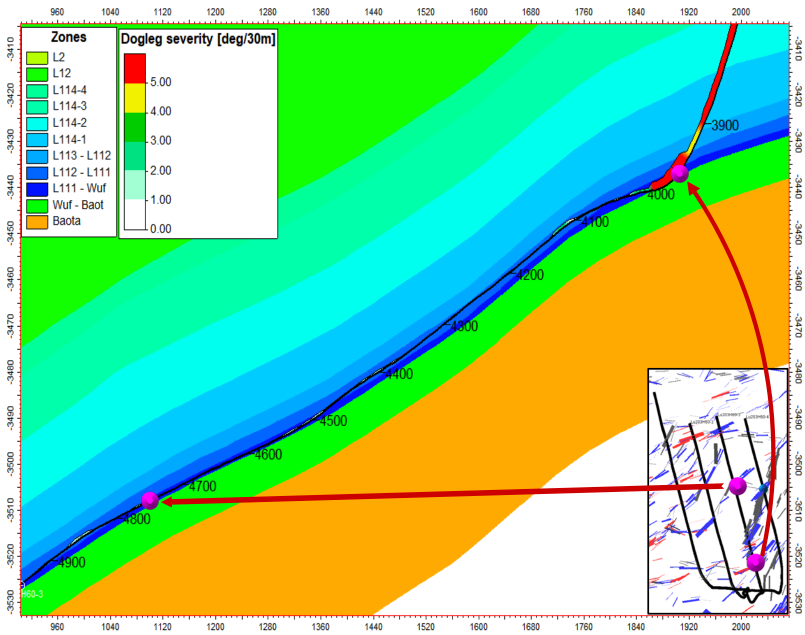

Figure 15. Comparison of casing deformation position, horizon and dogleg degree of well Lu 203H60-3.

7. Expectation

As mentioned above, many researches have been carried out on the mechanism of casing deformation, but some are not thorough enough. For example, some scholars believe that temperature is the main factor affecting the casing's compressive strength, but this view has not been proven. Perforation can destroy the integrity of the casing, but the deformation point of the casing is far from the perforation point. Currently, only field data support this idea, and the reason is not known. There are few studies on casing deformation caused by shale swelling and lifting formation, but shale water absorption and swelling occur in every stage of hydraulic fracturing. There are few countermeasures against these factors, most of which are based on numerical simulation and lack of physical experimental verification. On the other hand, the future is a time of both opportunities and challenges. In particular, the industry is moving toward big data. For example, when the influence of multiple factors makes it difficult to determine the primary mechanism of casing deformation, sensitivity analysis can make the ranking method more reliable and enable the recommendation of countermeasures [22,59,60]. Shale welling will raise the formation. Abbaszadeh Shahri [61] and Ghaderi [62] proposed that 3D models can be built to map the soil and predict future events so that they can accurately locate the casing deformation point. As mentioned earlier, hydraulic fracturing contributes to casing deformation. However, fracture extension is a complex process. Jin [59] proposes to monitor cracks based on DAS signals to avoid the uncertainty of traditional monitoring methods, and Huang [60] proposes a series of geological models to predict the fracture network. Abbaszadeh Shahri [63] proposes a state-of-the-art method (ARDCW) to integrate multiple models for visual estimation and exhibit superior capabilities. Then applying this technique to the petroleum engineering industry may have positive aspects. In short, the opportunities are enormous, and using artificial intelligence and big data analytics could lead to a dramatic shift in the oil and gas industry.

8. Conclusions

This work analyzed the associated developments in casing deformation. The author researched casing deformation characteristics, critical issues affecting casing deformation, and the relationships between various influence factors. In addition, effective countermeasures to casing deformation were highlighted. Based on our research, the following conclusions can be drawn:

(1) Casing deformation frequently occurs in shale gas development in the Sichuan Basin. The probability of casing deformation is the largest at target "A", and shear deformation is dominant, especially in the Changning-Weiyuan-Luzhou, since the area's geological structure is poor owing to natural fracture/fault and lithological interface development, and they are easily induced to slip. Furthermore, the natural fracture/fault and lithological interface are the main factors leading to casing deformation. Analysis shows that the casing deformation of the Lu 203H60-3 well is mainly caused by the bedding interface and fracture sliding.

(2) Although significant progress has been made in research on the mechanism of casing deformation in shale gas horizontal wells during hydraulic fracturing, at present, casing deformation cannot be sufficiently resolved, implying that the present understanding of its mechanism has not yet reached a significant level of maturity.

(3) Considering the effects of stress concentration and running casing, reducing casing deformation by increasing the wall thickness and grade of the casing is not optimal. By contrast, well trajectory optimization, cementing optimization, hydraulic fracturing parameter optimization, and shale inhibitor optimization are more desirable and operational.

(4) It is challenging to prevent casing deformation only by one preventive measure, so combining multiple measures is necessary to compensate for each other's shortcomings.

(5) Experiments on physical models can be used to verify the addition of nonuniform stress by cement voids on casings. At present, the results of research into casing deformation are based on numerical simulations and lack experimental research. If numerical simulations are combined with experimental research, more accurate research results should be obtained. The development of big data and artificial intelligence will provide new directions for casing deformation prevention.

Author Contributions: Methodology: B.X.; Writing-reviewing and editing: S.Y.; Writing-Original draft preparation: B.Y.; Data statistics and Language check: L.M.; Data curation: L.W. All authors have read and agreed to the published version of the manuscript.

Funding: The authors would like to acknowledge that this work was completed through financial support from the Natural Science Foundation National Science, Technology Major Project of China (2016ZX05002004-012).

Conflicts of Interest: The authors declare no conflict of interest.

References

1. Wang, Y.; Xu, S.; Hao, F.; Lu, Y.; Shu, Z.; Yan, D.; Lu, Y. Geochemical and petrographic characteristics of Wufeng-Longmaxi shales, Jiaoshiba area, southwest China: Implications for organic matter differential accumulation. *Mar. Pet. Geol.* **2019**, *102*, 138–154. [CrossRef]
2. Gao, J.; Zhang, J.-K.; He, S.; Zhao, J.-X.; He, Z.-L.; Wo, Y.-J.; Feng, Y.-X.; Li, W. Overpressure generation and evolution in Lower Paleozoic gas shales of the Jiaoshiba region, China: Implications for shale gas accumulation. *Mar. Pet. Geol.* **2019**, *102*, 844–859. [CrossRef]
3. Feng, Z.; Dong, D.; Tian, J.; Wu, W.; Cai, Y.; Shi, Z.; Peng, W. Geochemical characteristics of Lower Silurian shale gas in the Changning-Zhaotong exploration blocks, southern periphery of the Sichuan Basin. *J. Pet. Sci. Eng.* **2019**, *174*, 281–290. [CrossRef]
4. Xie, J. Rapid shale gas development accelerated by the progress in key technologies: A case study of the Changning–Weiyuan National Shale Gas Demonstration Zone. *Nat. Gas Ind. B* **2018**, *5*, 283–292. [CrossRef]
5. Wang, Q.; Wang, T.; Liu, W.; Zhang, J.; Feng, Q.; Lu, H.; Peng, P.A. Relationships among composition, porosity and permeability of Longmaxi Shale reservoir in the Weiyuan Block, Sichuan Basin, China. *Mar. Pet. Geol.* **2019**, *102*, 33–47. [CrossRef]
6. Zhai, G.-Y.; Wang, Y.-F.; Zhou, Z.; Yu, S.-F.; Chen, X.-L.; Zhang, Y.-X. Exploration and research progress of shale gas in China. *China Geol.* **2018**, *1*, 257–272. [CrossRef]
7. Guo, T.; Zhang, S.; Zou, Y.; Xiao, B. Numerical simulation of hydraulic fracture propagation in shale gas reservoir. *J. Nat. Gas Sci. Eng.* **2015**, *26*, 847–856. [CrossRef]
8. Yuan, B.; Wang, Y.; Zeng, S. Effect of slick water on permeability of shale gas reservoirs. *J. Energy Res. Technol.* **2018**, *140*, 112901–112907. [CrossRef]
9. Chen, Z.; Liao, X.; Zhao, X.; Dou, X.; Zhu, L. Performance of horizontal wells with fracture networks in shale gas formation. *J. Pet. Sci. Eng.* **2015**, *133*, 646–664. [CrossRef]
10. Yuan, B.; Zheng, D.; Moghanloo, R.G.; Wang, K. A novel integrated workflow for evaluation, optimization, and production predication in shale plays. *Int. J. Coal Geol.* **2017**, *180*, 18–28. [CrossRef]
11. Liu, Y.; Chen, C.; Ma, T.; Zhu, G.; Peng, N.; Zhang, X. Experimental Investigation on the Initiation of Hydraulic Fractures from a Simulated Wellbore in Laminated Shale. *Lithosphere* **2021**, *2021*, 4152918. [CrossRef]
12. Abbaszadeh Shahri, A.; Rezaei, F.; Mehdizadeh Farsad, S.; Mehdizadeh Farsad, K.; Panaei, N. Investigation of Engineering Geology Parameters in Creation of Hydraulic Fracturing in Order to Enhance Oil Recovery from Oil Reservoir Using Finite Element Method. *Sci. Q. J. Geosci.* **2015**, *24*, 3–9. [CrossRef]
13. Zhou, D.; Yang, H.; Jianjun, L.; Wang, X.; Wang, H.; Xue, Y. A test method for the in-situ stress of salt rock. *Oil Gas Storage Transp.* **2017**, *36*, 1385–1390. [CrossRef]
14. Yan, W.; Zou, L.; Li, H.; Deng, J.; Ge, H.; Wang, H. Investigation of casing deformation during hydraulic fracturing in high geo-stress shale gas play. *J. Pet. Sci. Eng.* **2017**, *150*, 22–29. [CrossRef]
15. Wang, W.; Zhang, H.; Liu, P.; Li, Z.; Ni, W.; Uechi, H.; Matsumura, T. A finite element method approach to the temperature distribution in the inner casing of a steam turbine in a combined cycle power plant. *Appl. Therm. Eng.* **2016**, *105*, 18–27. [CrossRef]
16. Liao, S.; Yu, S.; Yi, S.; Bo, Z.; Wang, L.; Lei, Y. Research and field tests of staged fracturing technology for casing deformation section in horizonta shale gas wells. *Nat. Gas Ind.* **2017**, *37*, 40–45. [CrossRef]
17. Qian, B.; Yin, C.; Li, Y.; Xu, B.; Qin, G. Diannostics of caing deformation in multistage hydraulic fracturing stimulation in lower Silurian Marine shale play in Southwestern China. In Proceedings of the Unconventional Resources Technology Conference, San Antonio, TX, USA, 20–22 July 2015; pp. 1–119.
18. Xi, Y.; Li, J.; Liu, G.; Zeng, Y.; Li, J. Ooverview of casing deformation in multistage fracturing of shale gas horizontal wells. *Spec. Oil Gas Reserv.* **2019**, *26*, 1–6. [CrossRef]
19. Xi, Y.; Li, J.; Liu, G.; Cha, C.; Fu, Y. Numerical investigation for different casing deformation reasons in Weiyuan-Changning shale gas field during multistage hydraulic fracturing. *J. Pet. Sci. Eng.* **2018**, *163*, 691–702. [CrossRef]
20. Guo, X.; Li, J.; Liu, G.; Xi, Y.; Zeng, Y.; He, M.; Yan, H. Numerical simulation of casing deformation during volume fracturing of horizontal shale gas wells. *J. Pet. Sci. Eng.* **2019**, *172*, 731–742. [CrossRef]
21. Chen, Z.; Shi, L.; Xiang, D. Mechanism of casing deformation in the Changning–Weiyuan national shale gas demonstration area and countermeasures. *Nat. Gas Ind. B* **2017**, *4*, 1–6. [CrossRef]
22. Xu, Z.; Yin, F.; Han, L.; Yang, S.; Wu, X. Mechanism study of casing deformation in multistage hydraulic fracturing shale reservoir. In Proceedings of the SPE/AAPG/SEG Unconventional Resources Technology Conference, Houston, TX, USA, 23–25 July 2018.
23. Yin, F.; Xiao, Y.; Han, L.; Wu, X. Quantifying the induced fracture slip and casing deformation in hydraulically fracturing shale gas wells. *J. Nat. Gas Sci. Eng.* **2018**, *60*, 103–111. [CrossRef]
24. Xi, Y.; Liu, G.; Li, J.; Zha, C.; Chao, W.; Liu, M. Calculation of wellbore temperature and analysis of its effect on casing strength during volume fracturing in shale gas well. *Fault Block Oil Gas Field* **2017**, *24*, 561–564. [CrossRef]

25. Wang, J.; Rao, X.; Han, L.; Li, Y.; Zhou, l.; Lu, X. Selection criteria and evaluation technology for casing used in shale gas wells in China. In Proceedings of the SPE Asia Pacific Unconventional Resources Conference and Exhibition, Brisbane, Australia, 9 November 2015; p. 10.
26. Jia, Z.; Liu, S.; Geng, Y.; Wang, M.; Ji, B. Theoretical and experimental study on the collapse strength of casing in curved well section. *China Pet. Mach.* **2018**, *46*, 100–105. [CrossRef]
27. Kaldal, G.S.; Jonsson, M.T.; Palsson, H.; Karlsdottir, S.N. Structural modeling of the casings in high temperature geothermal wells. *Geothermics* **2015**, *55*, 126–137. [CrossRef]
28. Wang, Z.; Ma, Z. Effect by thermal well temperature on casing properties and calculation method for pretension. *Steel Pipe* **2007**, *36*, 24–27. [CrossRef]
29. Yin, H.; Zhang, Y. A quantitative evaluation method for the effect of temperature on casing collapsing strength: A case study of large-scale hydraulic fracturing in shale gas horizontal wells. *Nat. Gas Ind.* **2016**, *36*, 73–77. [CrossRef]
30. Song, X.; Li, J.; Liu, G.; Xi, Y.; Lian, W.; Guo, X. Casing wear and stress distribution under coupling effects of temperature and pressure. *Fault Block Oil Gas Field* **2018**, *25*, 670–674. [CrossRef]
31. Lian, Z.; Yu, H.; Lin, T.; Guo, J. A study on casing deformation failure during multi-stage hydraulic fracturing for the stimulated reservoir volume of horizontal shale wells. *J. Nat. Gas Sci. Eng.* **2015**, *23*, 538–546. [CrossRef]
32. Zhao, C.; Li, J.; Liu, G.; Zhang, H.; Wang, C.; Ren, K.; Zhang, X. The casing deformation during shale gas hydraulic fracturing: Why it is so serious in weiyuan-changning, China? In Proceedings of the SPE Trinidad and Tobago Section Energy Resources Conference, Port of Spain, Trinidad and Tobago, 25–26 June 2018.
33. Liu, K.; Gao, D.; Wang, Y.; Liu, Y. Effects of local load on shale gas well casing deformation. *Nat. Gas Ind.* **2016**, *11*, 76–82. [CrossRef]
34. Guohua, W.; Zhengmao, C.; Jiyou, X.; Keli, Y. Study on the Effect of Non-Uniformity Load and Casing Eccentricity on the Casing Strength. *Energy Procedia* **2012**, *14*, 285–291. [CrossRef]
35. Liu, W.; Tao, C.; Wan, Y.; Chi, X.; LI, Y.; Lin, H.; Dend, J. Numerical analysis of casing deformation during massive hydraulic fracturing of horizontal wells in a tight-oil reservoir. *Pet. Sci. Bull.* **2017**, *2*, 466–477. [CrossRef]
36. Guo, X.; Li, J.; Liu, G.; Lian, W.; Zeng, Y.; Tao, Q.; Song, X. Shale experiment and numerical investigation of casing deformation during volume fracturing. *Arab. J. Geosci.* **2018**, *11*, 723. [CrossRef]
37. Li, H.; Li, Z.; Li, G.; Yu, H.; Jiang, Z.; He, L.; Guo, B.; Dong, M. Casing deformation mechanisms of horizontal wells in Weirong shale gas field during multistage hydraulic fracturing. *J. Nat. Gas Sci. Eng.* **2020**, *84*, 103646. [CrossRef]
38. He, Y.-Y.; Zhang, B.-P.; Duan, Y.-T.; Xue, C.-J.; Yan, X.; He, C.; Hu, T.-Y. Numerical simulation of surface and downhole deformation induced by hydraulic fracturing. *Appl. Geophys.* **2014**, *11*, 63–72. [CrossRef]
39. Bao, X.; Eaton, D.W. Fault activation by hydraulic fracturing in western Canada. *Science* **2016**, *354*, 1406–1409. [CrossRef]
40. Xi, Y.; Li, J.; Liu, G.; Zha, C.; QIin, X.; Yan, P. Impact analysis of cement sheath shape on casing stress under transient mechanical-thermal coupling effect. *Fault Block Oil Gas Field* **2017**, *24*, 700–704. [CrossRef]
41. Li, Z.; Li, H.; Li, G.; Yu, H.; Jiang, Z.; Liu, H.; Hu, S.; Tang, B. The influence of shale swelling on casing deformation during hydraulic fracturing. *J. Pet. Sci. Eng.* **2021**, *205*, 108844. [CrossRef]
42. Panjwani, S.; McDaniel, J.; Nikolaou, M. Improvement of zonal isolation in horizontal shale gas wells: A data-driven model-based approach. *J. Nat. Gas Sci. Eng.* **2017**, *47*, 101–113. [CrossRef]
43. Choueiri, G.H.; Tavoularis, S. Experimental investigation of flow development and gap vortex street in an eccentric annular channel. Part 1. Overview of the flow structure. *J. Fluid Mech.* **2014**, *752*, 521–542. [CrossRef]
44. Jiang, K.; Li, Q.; Chen, Y.; Guo, X.; Fu, Y.; Li, J. Influence of cementing quality on casing failures in horizontal shale gas wells. *Nat. Gas Ind.* **2015**, *35*, 77–82.
45. Yin, F.; Han, L.; Yang, S.; Deng, Y.; He, Y.; Wu, X. Casing deformation from fracture slip in hydraulic fracturing. *J. Pet. Sci. Eng.* **2018**, *166*, 235–241. [CrossRef]
46. Liu, S.; Li, D.; Yuan, J.; Qi, F.; Shen, J.; Guo, M. Cement sheath integrity of shale gas wells: A case study from the Sichuan Basin. *Nat. Gas Ind. B* **2018**, *5*, 22–28. [CrossRef]
47. Shi, X.; He, Z.; Long, S.; Peng, Y.; Li, D.; Jiang, S. Loading rate effect on the mechanical behavior of brittle longmaxi shale in nanoindentation. *Int. J. Hydrog. Energy* **2019**, *44*, 6481–6490. [CrossRef]
48. Liu, K.; Gao, D.; Taleghani, A.D. Analysis on integrity of cement sheath in the vertical section of wells during hydraulic fracturing. *J. Pet. Sci. Eng.* **2018**, *168*, 370–379. [CrossRef]
49. Liu, K.; Gao, D.; Wang, Y.; Yang, Y. Effect of local loads on shale gas well integrity during hydraulic fracturing process. *J. Nat. Gas Sci. Eng.* **2017**, *37*, 291–302. [CrossRef]
50. Zhang, B.; Guan, Z.; Hasan, A.R.; Lu, N.; Wang, Q.; Xu, Y.; Zhang, Q.; Liu, Y. Development and design of new casing to mitigate trapped annular pressure caused by thermal expansion in oil and gas wells. *Appl. Therm. Eng.* **2017**, *118*, 292–298. [CrossRef]
51. Wu, Y.; Cheng, L.; Huang, S.; Jia, P.; Zhang, J.; Lan, X.; Huang, H. A practical method for production data analysis from multistage fractured horizontal wells in shale gas reservoirs. *Fuel* **2016**, *186*, 821–829. [CrossRef]
52. Yu, H.; Dahi Taleghani, A.; Lian, Z. On how pumping hesitations may improve complexity of hydraulic fractures, a simulation study. *Fuel* **2019**, *249*, 294–308. [CrossRef]
53. Zhang, H.; Chen, Z.; Shi, l.; Xiang, D.; Wang, S.; Wang, Q.; Zhou, L. Mechanism of how fluid passage formed and application in sichuan shale gas casing deformation analysis. *Drill. Prod. Technol.* **2018**, *41*, 8–11. [CrossRef]

54. Velayati, A.; Roostaei, M.; Rasoolimanesh, R.; Soleymani, M.; Fattahpour, V. Colloidal gas aphron (CGA) based foam cement system. *Pet. Explor. Dev.* **2019**, *46*, 1281–1287. [CrossRef]
55. Zhang, P.; He, Y.; Liu, Z.; Tong, H.; Deng, C.; Ren, X.; Zhang, H.; Li, Y.; Qu, L.; Fu, Q.; et al. Shear compression deformation test and deformation prevention practice of casing in shale gas horizontal wells. *Nat. Gas Ind. B* **2021**, *8*, 514–522. [CrossRef]
56. Li, L.; Wang, G.; Lian, Z.; Zhang, L.; Mei, J.; He, Y. Deformation mechanism of horizontal shale gas well production casing and its engineering solution: A case study on the Huangjinba Block of the Zhaotong National Shale Gas Demonstration Zone. *Nat. Gas Ind. B* **2018**, *5*, 261–269. [CrossRef]
57. Quainoo, A.K.; Negash, B.M.; Bavoh, C.B.; Ganat, T.O.; Tackie-Otoo, B.N. A perspective on the potential application of bio-inhibitors for shale stabilization during drilling and hydraulic fracturing processes. *J. Nat. Gas Sci. Eng.* **2020**, *79*, 103380. [CrossRef]
58. Wang, B.; Liu, B.; Yang, J.; Bai, L.; Li, S. Compatibility characteristics of fracturing fluid and shale oil reservoir: A case study of the first member of Qingshankou Formation, northern Songliao Basin, Northeast China. *J. Pet. Sci. Eng.* **2022**, *211*, 110161. [CrossRef]
59. Jin, G.; Roy, B. Hydraulic-fracture geometry characterization using low-frequency DAS signal. *Lead. Edge* **2017**, *36*, 975–980. [CrossRef]
60. Huang, J.; Safari, R.; Mutlu, U.; Burns, K.; Geldmacher, I.; McClure, M.; Jackson, S. Natural-Hydraulic Fracture Interaction: Microseismic Observations and Geomechanical Predictions. In Proceedings of the SPE/AAPG/SEG Unconventional Resources Technology Conference, Denver, CO, USA, 25–27 August 2014. [CrossRef]
61. Abbaszadeh Shahri, A.; Kheiri, A.; Hamzeh, A. Subsurface Topographic Modeling Using Geospatial and Data Driven Algorithm. *ISPRS Int. J. Geo-Inf.* **2021**, *10*, 341. [CrossRef]
62. Ghaderi, A.; Abbaszadeh Shahri, A.; Larsson, S. A visualized hybrid intelligent model to delineate Swedish fine-grained soil layers using clay sensitivity. *CATENA* **2022**, *214*, 106289. [CrossRef]
63. Abbaszadeh Shahri, A.; Shan, C.; Larsson, S. A Novel Approach to Uncertainty Quantification in Groundwater Table Modeling by Automated Predictive Deep Learning. *Nat. Resour. Res.* **2022**, *31*, 1351–1373. [CrossRef]